The EMBO Journal vol.13 no.2 pp.318-326, 1994

Fine structure of influenza A virus observed by electron cryo-microscopy

Yoshinori Fujiyoshi[3], Nahoaki P.Kume[1], Kazumi Sakata and Satoshi B.Sato[2]

Protein Engineering Research Institute 6-2-3, Furuedai, Suita, Osaka 565 and [1]Cryogenic Laboratory and [2]Department of Biophysics, Faculty of Science, Kyoto University, Kyoto 606, Japan

[3]Corresponding author

Communicated by E.F.J.van Bruggen

A rapidly frozen vitrified aqueous suspension of influenza A virus was observed by high resolution electron cryo-microscopy. The influenza particles were grouped into small (diameter <150 nm) spherical particles with well organized interiors, large spherical ones with less internal organization, and filamentous ones. Envelopes of most of the large virus particles were phospholipid bilayers, and the chromatography fraction containing these large particles was largely devoid of viral activity. The envelopes of most of the filamentous and small spherical virus particles, on the other hand, gave a strange contrast which could be ascribed to a combination of a thin outer lipid monolayer and a 7.2 nm thick protein-containing inner layer. These latter particles represented most of the viral activity in the preparation. Densitometric traces of the near in-focus images confirmed these structural differences. Some viral envelope structures apparently intermediate between these two distinct types of membrane were also detected. A structural model of intact biologically active influenza virus particles was formulated from these results, together with computer simulations.

Key words: glycoprotein/lipid/matrix protein/membrane/RNA-protein complexes

Introduction

Numerous studies of influenza virus have already achieved the functional characterization of its eight segmented RNAs and seven structural and several non-structural proteins, as shown in reviews (Lamb and Choppin, 1983; Oxford and Hockley, 1987). The arrangement of each component in the virus particle has also been studied by many biophysical and biochemical methods. In particular, electron microscopic methods have made an important contribution towards providing an understanding of the ultrastructure of the components and their organization in influenza particles as shown in the comprehensive review by Wrigley *et al.* (1986). Low resolution structures of the membrane bound glycoproteins: haemagglutinin (HA) and neuraminidase (NA); and of the internal RNA-protein complexes involving P proteins (PA, PB1 and PB2) and nucleoprotein (NP), as well as some features of matrix (M) protein, have all been investigated by various electron microscopic methods. In addition, high resolution structures of HA and NA (in each instance, minus their cytoplasmic and membrane spanning regions) have been analyzed by X-ray crystallography (Wiley *et al.*, 1981; Colman *et al.*, 1983, respectively).

The structure of the virus is regarded as sharing some parts of a host cell because the virus behaves as if it were an intrinsic component of the host cell from its entry to budding, and the formation of the virus particles is the result of the modification of the host cell structure. This has led to conjecture that the viral membrane should have a lipid bilayer structure equivalent to that of the membrane of the host cell. On this basis, Nermut (1972) interpreted his electron micrographs from positively stained ultrathin sections of influenza virus strain X-31 and proposed a model diagram of a combination of a lipid bilayer and a core-membrane layer for the viral surface structure. However, the native non-dehydrated structure of the influenza particle itself still remains to be elucidated at high resolution.

The advent of electron cryo-microscopy has brought about an important advance in the study of the intact architecture of biological specimens. By rapid freezing of a thin film of a virus suspension and using a cryo-transfer-holder cooled with liquid nitrogen to prevent devitrification of the frozen specimen, native fully hydrated viruses were first successfully observed by Adrian *et al.* (1984). Booy *et al.* (1985) later examined native purified, inactivated type B influenza virus and crude type A influenza virus in a similar microscope.

Although electron cryo-microscopy enables observation of intact biological structures and is important for independently evaluating the interpretation of stained specimens, sometimes the images obtained with the electron cryo-microscope have not been distinct in their detail and have not attained a sufficiently high resolution for discriminating complex molecular assemblies. For non-stained biological materials, especially non-crystalline ones, the resolution of their electron micrographs has been restricted principally by irradiation damage.

Cooling of the biological specimen is emerging as the most promising approach to reducing the irradiation damage. We have developed a high resolution electron cryo-microscope capable of observing specimens at liquid helium temperature (Fujiyoshi *et al.*, 1991). This electron cryo-microscope routinely attains a resolution of up to 0.26 nm at a specimen-stage temperature of 1.5 K. In addition, we have also developed a new cryo-transfer system for the high resolution top-entry specimen-stage of the microscope (Fujiyoshi *et al.*, 1986). The reliability as well as ease of operation of this microscope offers the opportunity for a non-expert to record high resolution micrographs of radiation sensitive biological materials in the frozen-hydrated state.

Using this high resolution electron cryo-microscope, we have now investigated the ultrastructure of two intact influenza A viruses and compared the results with those of earlier reports.

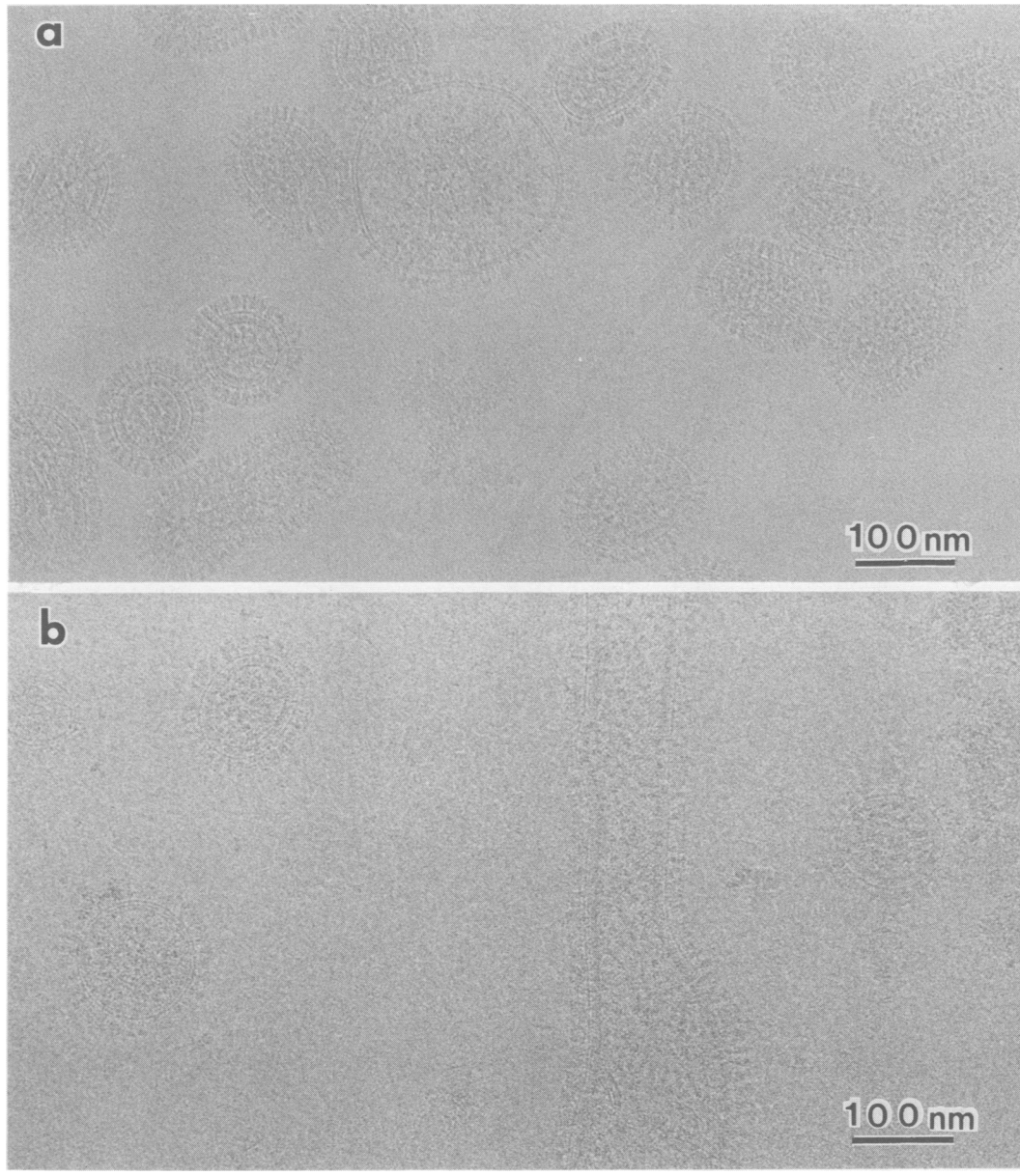

Fig. 1. High resolution electron micrographs of influenza virus A/PR/8/34 (**a**) and X-31 (**b**) particles embedded in vitreous ice. For details see text.

Results

Images of the fine structure of influenza particles

We examined two well characterized influenza virus type A strains, A/PR/8/34 and X-31. Micrographs recorded at 4.2 K at a magnification of 40 000× with an accelerating voltage of 400 kV are shown in Figure 1. A defocus setting of ~100 nm under focus was employed for Figure 1a and ~90 nm under focus for Figure 1b, each at a dose of 4000 electrons/nm^2.

The signal:noise ratio and resolution of the images were remarkably improved compared with those in the earlier reports of electron cryo-microscopy of viruses. The resolution limit was estimated to be 1.4 nm when checked via the optical transform of an image of amorphous carbon film taken under the same conditions as these images.

The glycoprotein spikes were easily recognized on the viral envelopes, thereby identifying unequivocally the influenza particles within the specimen. The purified virus particles could be roughly grouped into three types as previously reported (Wrigley *et al.*, 1986). These were small (<150 nm diameter) spherical particles well organized internally, one less well organized larger, spherical particle, and filamentous or rod shaped, non-spherical particles.

In the small virus particles, the boundary between the inner assembly which would be RNA–protein complex and the outer structure was clearly recognizable. In some cases we could detect free RNA–protein complexes released from broken virus particles, in which an RNA molecule formed two nearly parallel lines with ~5.0 nm overall width, with nucleoproteins of diameter also ~5 nm bound to the RNA at intervals of ~10 nm (Figure 2a). Rod shaped structures of ~17 nm diameter were observed within intact virus particles from which the surface proteins had been cleaved by bromelain (Brand and Skehel, 1972) to allow the internal ribonucleoprotein coils to be observed without the superposition of image contrast from the surface spike proteins (Figure 2b). These internal structures within the virus have a very similar appearance to that reported by Pons *et al.* (1969).

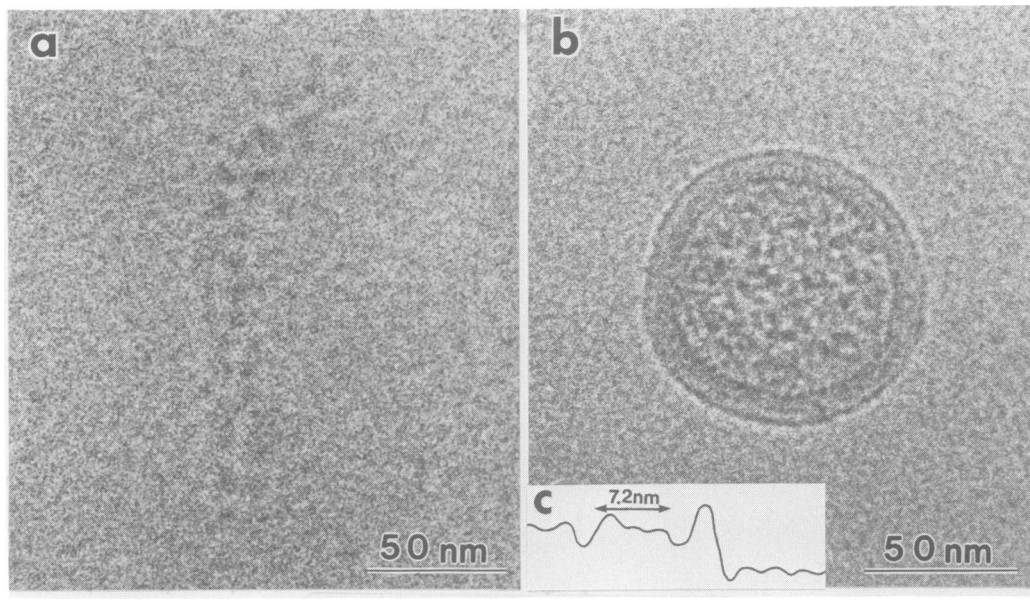

Fig. 2. A free RNA–protein complex released from a broken influenza particle (**a**). A small intact A/PR/8/34 particle treated with bromelain (**b**) and a densitometric trace of the envelope of the bromelain treated particle (**c**). We can observe, in (a), two parallel beads of RNA–protein complex of overall width ~17 nm, and in (b), a nucleoprotein coiled stem also ~17 nm thick.

Image contrast of the viral envelope

In many influenza particles, especially small compact ones, the envelopes were found not to be a simple coupling of two phospholipid layers: we could detect only a single dark line on the viral envelope (Figures 1 and 2b); underneath was a moderately dense lining ~7.2 nm thick which wrapped the inner-core structure of the virus. As shown in Figure 1, almost all the small compact virus particles had this new type of membrane as their envelope. This composite membrane structure was also consistently observed after the surface-spike proteins were cleaved by bromelain as shown in Figure 2b. In addition, in small intact particles from which the HA and NA had been cleaved, finer details of the viral envelope could be scrutinized more carefully without superposition of projected detail from surface proteins.

Without exception, filamentous influenza particles also possessed this new type of membrane (Figure 1b). In contrast, in the large virus particles, two dark lines were clearly distinguishable with a separation of ~3.8 nm. No thick underlying structure was evident. These two types of membrane structure are observed in the same photographs as shown in Figure 1a and b.

Besides these two types of membrane, we detected, but appreciably less frequently (<5% of the total number of virus particles), apparently intermediate membrane structures. These membranes gave image contrasts of two dark lines and an underlying moderately dense lining either 3 or 5 nm thick. The appearance of these membranes differed from particle to particle among this intermediate group. In some cases, the thickness of the moderately dense lining changed within a single virus particle. In such a particle, some areas of the membrane gave a contrast pattern of two dark lines and a moderately dense lining ~3 nm thick, and other areas gave a pattern of only two dark lines without any moderately dense lining as shown in Figure 3a. In other particles, an area would display a contrast pattern of two dark lines and a moderately dense lining ~5 nm thick, whilst in the bordering areas the inner dark line would disappear, merging into the composite membrane as shown in Figure 3b. Most of these intermediate structures were detected in intermediate sized particles ranging from 100 to 400 nm in diameter. These intermediate structures could easily be distinguished from the consistent contrast pattern of a single dark line plus a 7.2 nm thick moderately dense lining in the viral envelopes of small influenza particles. All of these intermediate membrane structures were always detected, both in samples observed just after preparation and in frozen stored ones.

After obtaining this result, several other biological membranes as well as many kinds of liposomes were examined. These included human erythrocyte ghosts, nuclear membranes of rat hepatocytes, the microsome fraction of cultured cells, sonicated pure lipid vesicles and large unilamellar vesicles prepared by reverse-phase evaporation (Szoka and Papahadjopoulos, 1978). All of these membranes showed the typical contrast pattern of two dark lines representing phospholipid bilayers (data not shown).

Characterization of small and large influenza particles

Using Sephacryl S-1000 chromatography, the sucrose gradient purified influenza particles were separated into two peaks. Large particles were recovered in fractions near void volume and they were separated from small ones (data not shown). Typical images of large and small particles are shown in Figure 3c and d, respectively. Of total infectivity tested by plaque assay on chick embryo fibroblasts (5×10^{11} p.f.u./mg protein) 80–97% and most of the other activity indicators including fusion and haemagglutination were incorporated in the fractions containing small particles. By SDS–PAGE, we found that the small virus particles contained all the structural proteins without any host cell components even after extensive silver staining, but small amounts of other protein bands were detected in the fraction containing the larger particles. We concluded that the small virus particles disproportionately

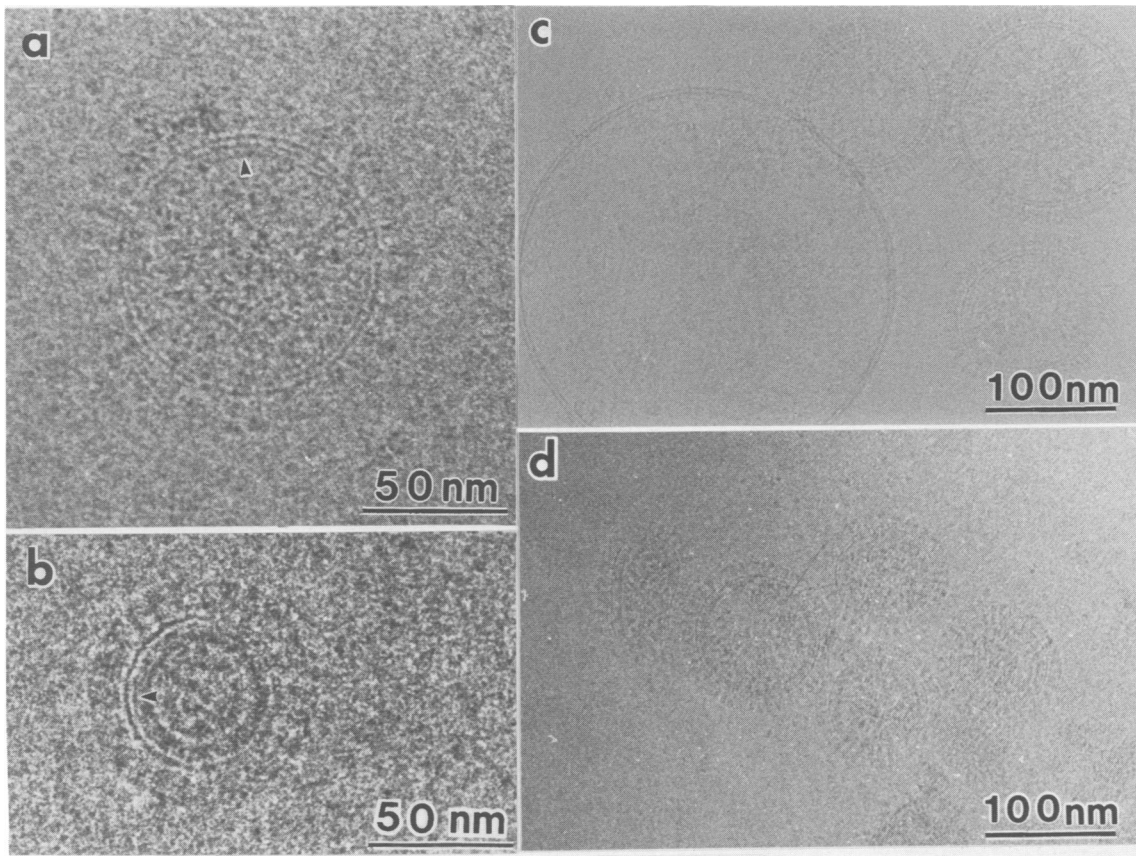

Fig. 3. Influenza virus envelopes containing a thin layer of 3.8 nm width beneath a lipid bilayer (**a**) (arrowhead), and a thick layer of 7.2 nm width beneath a lipid single layer (**b**). An area of lipid bilayer without any protein layer can be observed in (a), and a region where the inner half of a lipid bilayer can be observed within the thick virus envelope is indicated by an arrowhead in (b). These images (a and b) are typical examples of the range of structures of the viral envelope intermediate between the lipid single layer plus moderately dense lining and the lipid bilayer. Typical images of large particles (**c**) and small particles (**d**) separated by Sephacryl S-1000 chromatography.

Table I. Characterization of small and large influenza particles

	HAU[a]	Hemolysis[b] (mg)	Fusion[c]	Protein:lipid ratio[d]	HA[e]	M/HA[f]
Small particles	234 400	15	29.5	7.80	1	0.76
Large particles	18 300	35	7.0	6.56	0.63	0.43
Ratio[g]	128	1/2.3	4.2	1.19	1.60	1.76

[a]Haemagglutination unit per 1 mg protein of influenza virus.
[b]Amount of protein which caused 50% of haemolysis of human erythrocytes.
[c]Percent of fusion of 3 μg protein of influenza virus with human erythrocyte ghosts at pH 5.2 in 20 min at 25°C.
[d]Protein and phospholipid were determined as in Materials and methods. Ratios are expressed in w/w, taking the mol. wt of phospholipids as 760.
[e]Equivalent quantities of protein from the two fractions were run on SDS−PAGE and the amounts of bound Coomassie dye in the HA bands were compared. The value for HA in the small particle fraction was taken as 1.
[f]The amount of M was measured as in e and the ratio of the bound dye in HA and M in each fraction was obtained.
[g]Ratio of the values for the small and the large particle fractions.

represented most of the biological activity of our influenza virus preparations.

The amounts of HA and M protein were determined by quantification of the SDS−PAGE gel. Using the same total quantity of protein in each fraction, the amounts of HA and M proteins in large particles corresponded to only 65 and 20%, respectively, of the amounts in small particles. This correlates with the finding that external spike proteins with an appearance very similar to that of HA were detected on almost all large particles, though less densely packed than on the surface of small particles (see Figure 1a or Figure 3c and d); on the other hand, the large particles were consistently virtually devoid of moderately dense inner lining as a discrete structural component of their viral envelope (although any M protein dispersed throughout the viral core would not have been recognized by our imaging techniques). The results are summarized in Table I.

Density profiles of the viral envelopes

In the present experiment with this electron microscope, the image was formed with electrons which passed through an objective aperture corresponding to a spatial frequency of 0.4 nm. The focusing condition used for recording these images rules out any significant modification of the images by the contrast-transfer function of the electron microscope (see Discussion). Figure 4 shows the near in-focus images

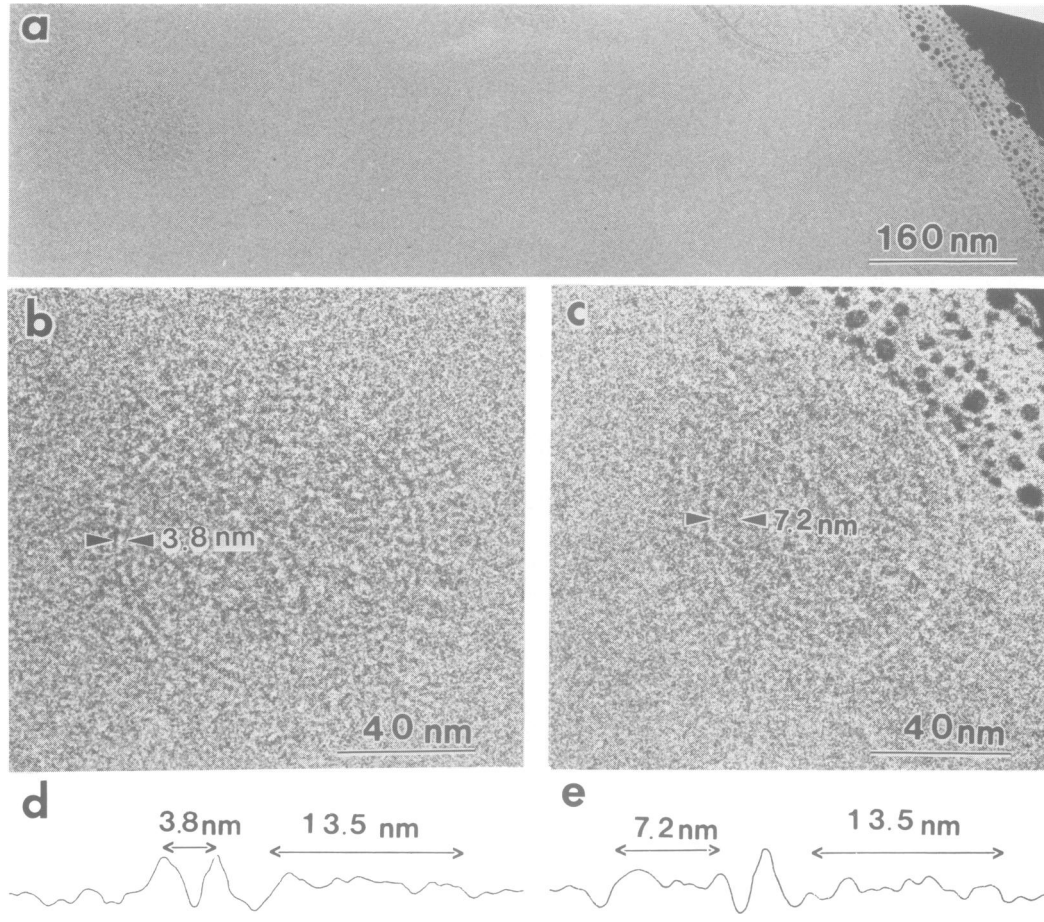

Fig. 4. Taken from the same field of view (**a**), in-focus electron microscopic images of two similarly sized influenza particles (A/PR/8/34) with different membrane structures (**b** and **c**) and the densitometric traces of their envelopes (**d** and **e**, respectively). The densitometric traces represent the right hand side of each of the illustrated particles, and in each case the 13.5 nm dimension represents the spike proteins extending beyond the outer surface of the viral envelope.

of two influenza particles with two distinct types of envelope. Since these images were printed from the same film (Figure 4a), all the conditions which contribute to imaging such as defocusing, astigmatism correction, image resolution, specimen-drift and specimen-thickness were the same, thereby eliminating these parameters as causal factors of image differences of influenza particles within a single field of view. In order to define more precisely the arrangement of molecular layers within the viral envelope, densitometric traces were taken from enlarged images on Sakura graphic art film.

Because the contrast-transfer function was not a significant modifying factor, we can obtain a densitometric profile which corresponds to the projected potential profile of the equatorial scan of a spherical membrane within the resolution limit of the image.

Particles of a similar size but with different membrane structures were selected because we were at first wary of possible size dependence of image contrast of the spherical membranes. However, we later found that the image contrast was little affected by the particle size under proper focusing conditions; on the other hand, it was severely distorted by the excess under-focusing typically used for enhancing the contrast of the image.

The densitometric trace of the two sharp dark envelope lines of the particle in Figure 4b showed two symmetrical high peaks corresponding to phosphates with a spacing of of 3.8 ± 0.2 nm (Figure4d). Between the peaks, there was an electron-translucent zone corresponding to the hydrocarbon chains of lipid. The overall profile was nearly symmetric. The profile is very similar to that obtained from the X-ray diffraction study of oriented multilamellar lipid membranes (Levine and Wilkins, 1971). In contrast, the two symmetrical high peaks were not detected in the trace of the newly discriminated membrane of the particle in Figure 4c: only a single dominant peak was detected in the outer periphery of the viral envelope (Figure 4e). This single peak density profile was almost the same as that of one half of the double peak profile in Figure 4d from the lipid bilayer membrane. No similarly high peak was detected in the inner thick leaflet. The thickness of the inner lining was 7.2 ± 0.2 nm. This layer was nearly four times thicker than the lipid monolayer. In both Figure 4d and e, the 13.5 nm feature of the density profile arose from the edge-projection of the HA and NA surface glycoproteins.

As shown in Figure 2c, the profile of a small particle treated with bromelain which removes the membrane bound surface glycoprotein was very similar to that of the intact particle (Figure 4e) except for the corresponding part of surface glycoproteins.

Computer simulation of the viral envelope

To interpret the electron micrographs and identify what has been observed, images of viral envelopes were simulated

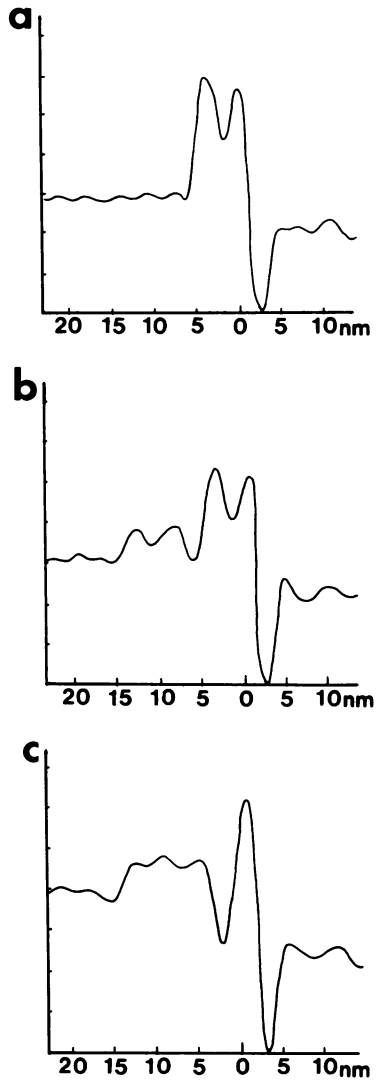

Fig. 5. Computer simulations of viral envelopes. Three envelopes were simulated under our experimental imaging conditions using the 'Multislice and Image-Simulation Programs', and then the sectional profiles were calculated for the three envelopes: typical lipid bilayer, lipid bilayer plus underlying protein layer and lipid single layer plus underlying protein layer, as shown in (**a**), (**b**) and (**c**), respectively.

by the 'Multislice and Image-Simulation Programs' developed by Ishizuka (1977). Three types of membrane structure, a typical lipid bilayer, a lipid bilayer plus an underlying protein layer and a lipid single layer plus an underlying protein layer, were simulated under the same electron-optical conditions as used in our imaging experiments.

Approximate models of the three types of membrane to be used in the simulations were constructed as cylindrical envelopes with a diameter of 100 nm composed of three atoms: carbon, oxygen and phosphorus. In these simulations, the cylindrical envelopes were surrounded by water. All atoms in the protein component were represented by carbon atoms, the coordinates of which were selected by random numbers to coincide with the density (1.3 g/cm^3) of the protein layer. The coordinates of lipid layer in the envelopes were calculated from the model structure of Figure 2.6 in Cevc and Marsh (1987). The coordinates of surrounding water were selected by random numbers to coincide with the density of water. The model structures were simulated in a large unit cell, such as 90 nm × 10 nm × 150 nm to minimize the boundary effect of the Fourier transformation. The simulated contrast was averaged on the central 4 nm regions of the cylindrical envelopes, and the sectional profiles were drawn. The results of the simulations indicated that the highest peaks in the contrast profiles of all three models would coincide with the spherical layers of phosphorus atoms as shown in Figure 5.

Discussion

We have obtained clear images of intact influenza virus at high resolution. The upper limit of resolution was estimated to be 1.4 nm. This resolution can be compared with that achieved by conventional high dose staining techniques which have an intrinsic limit of resolution not higher than ~2 nm. Our results are achieved both by reducing the mechanical instability of our electron cryo-microscope, and by reducing irradiation damage to the biological specimen. These advances are important for obtaining clear images of biological assemblies.

By using our high resolution electron cryo-microscope, two major influenza viral envelope structures were observed in the same micrographs as shown in Figure 1a and b and in Figure 4a. One structure displays a pair of parallel dark lines of spacing 3.8 nm as the viral envelope. For comparison with these observations on influenza particles, we observed several biological membranes and pure lipid vesicles which have been previously proposed to be bilayers by means of several lines of convincing experimental evidence. Without exception our observations of these alternative materials have depicted two clear concentric dark rings in our cryo-microscope. From these observations, and from the results of computer simulations of lipid bilayers, the pair of parallel lines in the large viral envelope was attributed to a phospholipid bilayer.

The other major observed structure gives a single dark line plus a moderately dense inner lining ~7.2 nm thick as the envelope of the small virion. This image contrast differs to a surprising degree from that of the lipid bilayer, and computer simulations indicate that this contrast pattern is impossible to achieve from a membrane structure of a lipid bilayer plus a protein layer. If the membrane has a composite structure of a lipid bilayer plus a protein layer, the simulated image would give a contrast pattern of two dark lines and a moderately dense inner lining. However, the computer simulation revealed that the experimentally observed contrast profile can only be achieved from a composite membrane structure of a lipid single layer plus a protein layer. In addition, the non-lipid bilayer appearance of the small virus particles and filamentous particles could be observed under a broad range of defocus conditions. Additionally, we could routinely discriminate between these two distinctly different membrane structures within any single micrograph, as depicted in Figures 1 and 4a.

As we have seen, the present fine structure images of the membranes of small biologically active influenza particles were not interpreted as being those of the usual phospholipid bilayer. Instead, they were interpreted as a single phospholipid layer plus a 7.2 nm thick protein-containing layer. This membrane structure contrasts with that of the lipid bilayer appearance in the large influenza particles. These latter images are not ascribed to any modification or

deterioration of the native structure either by the conditions of microscopic photographing or by the projection of the spherical particles on to the plane of the electron microscopic film in the electron microscope.

Booy *et al.* (1985) were the first to report cryo-microscopic images of influenza virus. They primarily examined β-propiolactone inactivated type B influenza virus. They concluded from those of their images recorded near in-focus that the membrane of the virus particle was a phospholipid bilayer. Their conclusion is at variance with our observation of type A influenza virus. By careful examination of their published results, we admit that the membranes they indicate in their micrographs are indeed bilayers. On the other hand, some of the particles in their published micrographs appear to be very similar to those we have observed. As there appears to be no good reason for the same structure to be photographed differently on the same cryo-micrograph within any single high resolution electron cryo-microscopic experiment, we believe unequivocally that two different envelope structures have actually been observed on the same copy of such photographs. Booy *et al.* (1985) also showed a photograph of a crude preparation of type A influenza virus, that of strain X-31. In their photograph, membranes of larger virus particles are actually lipid bilayers but on careful inspection we can point out the non-lipid bilayer envelopes in their images of small virus particles. We confirmed this by taking very similar images of X-31 particles at lower magnification and, to enhance the image contrast, in more defocused condition than in our present experiments. We should emphasize here that it was only after obtaining high resolution near in-focus images that we could discriminate between these different membrane structures in the highly defocused images.

Using conventional staining techniques, Nermut (1972) has made an extensive investigation of influenza virus membranes. He has shown photographs (Figures 17 and 18 of Nermut, 1972) clearly depicting a membrane appearance in a thin stained section of small influenza particles similar to that observed in the present study. He has also demonstrated the existence of a regular arrangement of proteins resembling a human thumbprint with spacing and thickness of 3.5 nm beneath the membrane-like structure. We also observed an apparently similar thumbprint-like structure with similar spacing (data not shown). However, in contrast to our analysis, he interpreted his results as a single layer of M protein 'core' surrounded by a lipid bilayer envelope. Such an interpretation was made by first adopting the lipid bilayer structure of the larger particles as a common structural element. However, we propose that the membrane structure of the large particles cannot be applied to that of the smaller ones. From our results, the membrane structures of small and large influenza particles are fundamentally different.

We assume that M protein [mol. wt = 27 861 (Winter and Fields, 1980)] is the only protein component of the thick protein–lipid lining coupled to the outer single phospholipid layer. Interaction of M protein with lipid bilayer membranes and the resulting modification of the membrane structure have been reported (Bucher *et al.*, 1980; Gregoriades, 1980). We sometimes detected apparently intermediate structures of membranes in which 3.8 or 5.3 nm thick proteinaceous material was intimately attached to the inner leaflet of a lipid bilayer (Figure 3a). These may be structures incompletely modified by M protein. Complete membrane modification and interaction with RNA–protein complexes would, in our interpretation, result in the formation of small compact active influenza particles.

Assuming the partial specific volume of protein to be 0.69–0.75 ml/g, the diameter of M protein as a globular protein molecule is estimated to be 3.9–4.0 nm. This value roughly corresponds to half of the lining thickness. If we take the diameter of influenza particles (excluding spikes) to be ~90 nm and the volume of M protein in the layer to be the same as that estimated for a globular protein of the above diameter, and assume that lipids occupy a similar volume within the inner protein–lipid layer to that in the outer lipid layer, the estimated number of protein molecules in the 7.2 nm thick layer per particle is calculated to range from 2500 to 2900. These values roughly agree with reported values of 2780 and 3170 (Compans *et al.*, 1970; Skehel and Schild, 1971, respectively) obtained by biochemical estimation. By contrast, in the case of the 3.8 nm layer which is suggested as the M protein 'core' by conventional microscopic methods (e.g. Nermut, 1972), the number of molecules of M protein as a globular protein with a diameter of 3.8 nm in an influenza particle of diameter 90 nm is ~1600.

Potential membrane spanning regions of HA and NA were predicted according to Klein *et al.* (1985), and the results indicated that the lengths of the significantly hydrophobic zones were 30 amino acid residues and 29 residues, respectively. Hydropathy plots, which were calculated by the method developed by Kyte and Doolittle (1982), also indicated such long potential membrane spanning regions for both spike proteins. Even if the whole of these hydrophobic zones of HA and NA were to adopt an α-helical conformation, which would give the shortest length to the secondary structures of these zones, the lengths of these 30 and 29 residue zones would be a minimum of 4.5 nm and 4.35 nm, respectively. Even the shorter of these is too large for spanning a simple lipid bilayer. This suggests that the tail regions of the hydrophobic zones of both spike proteins will extend appreciably beyond the single phospholipid monolayer to interact with hydrophobic parts of M proteins and/or the protein–lipid lining.

Although the interaction of influenza virus surface glycoproteins and M protein has not been well characterized, we suggest that the interaction may help the sieving of host cell membrane proteins out of the progeny virus particle. As influenza virus buds from the plasma membrane, the modification from a lipid bilayer to a lipid monolayer plus protein–lipid layer might not only perform this sieving function, but also be advantageous in overcoming the potential distortion of the ratio of lipids on the inner to the outer leaflets of the host cell plasma membrane during the formation of small compact virus particles with high surface curvature. Fuller (1987) has suggested a bent polyhedral structure for the lipid bilayer surrounding the nucleocapsid in Sindbis virus as a means of circumventing this latter problem of lipid packing: that virus, however, lacks any equivalent of an M-like protein.

For the formation of very compact small virus particles completely free from cellular proteins, there would need to be some mechanism for host cell membrane lipids to be incorporated into progeny virus particles without the

concomitant incorporation of host cell membrane proteins. As suggested above, extensive modification of the inner leaflet of the membrane bilayer may be such a mechanism for influenza particle formation. Much more study is needed to test this hypothesis. Because budding of influenza particles from host cell plasma membranes has been repeatedly observed (for example, Bächi *et al.*, 1969; Herrero-Uribe *et al.*, 1983), electron cryo-microscopy of frozen-hydrated sections of infected cells may well be one candidate method for studying the mechanism of influenza particle formation.

Although the following is presented here as a speculative discussion only, the model of the lipid single layer plus the moderately dense inner lining could require, during the formation of the viral envelope, a chaperone-like protein or chemical for preventing the aggregation of M protein molecules caused by one or more lipid-interacting hydrophobic regions on their surface. The chaperone-like protein could then be released at the formation of the inner protein−lipid layer of the viral envelope in much the same way as proposed for the secretion of HA protein and the formation of the HA trimer (Gething *et al.*, 1986). The M proteins of influenza A and B virus have been examined by various methods (e.g. Kyte and Doolittle, 1982; Nishikawa and Ooi, 1986) to assign hydrophobicity−hydrophilicity values to the residues in their known amino acid sequences (courtesy of Nishikawa), and it has emerged that they do in fact have many hydrophobic regions (data not shown). However, it is not known at this stage whether the M protein actually has any hydrophobic region on its surface or not.

In conclusion, a new model for the envelope of active (infective) influenza virus is proposed based on our observations of small intact frozen-hydrated type A influenza virus particles by high resolution electron cryo-microscopy. In this new model, an outer phospholipid monolayer and a thick inner layer couple together to form a hetero-complex as the viral envelope.

Materials and methods

Virus

Two strains of influenza virus, A/PR/8/34 and X-31, were propagated in 10 day old embryonated hen eggs and purified by differential centrifugation (Maeda and Ohnishi, 1980). The virus was further purified by 30−60% discontinuous sucrose density gradient centrifugation at 100 000 *g* for 90 min at 4°C. Purified virus was resuspended in TES−saline [10 mM Na *N*-Tris(hydroxymethyl)methyl-2-aminoethanesulfonate, 140 mM NaCl pH 7.4] and stored in liquid nitrogen if not used immediately. Sometimes the sucrose density gradient purified virus was further separated by Sephacryl S-1000 (Pharmacia) chromatography (1.5 × 85 cm at a flow rate of 10 ml/h at 4°C). Removal of the membrane bound surface glycoproteins HA and NA from the virus particles was done according to Brand and Skehel (1972).

Electron cryo-microscopy

The facility used in this study was a new high resolution electron cryo-microscope equipped with a cryo-transfer system, construction of which was based upon a standard JEOL JEM- 4000EX microscope (Fujiyoshi *et al.*, 1991). Influenza virus was embedded in a thin film of vitreous ice on a specimen grid using the Reichert−Jung KF-80 immersion cryo-fixation apparatus, employing liquid ethane at ~100 K as the coolant. The vitrified specimen was transferred into the microscope cryo-stage which was pre-cooled to 1.5 K with superfluid helium. The stage temperature was monitored by the temperature dependent change of electrical resistance of a Ge probe mounted in the cryo-stage. The temperature was then raised to 4.2 K in order to prevent stage vibration caused by turbulent flow of liquid helium (Fujiyoshi *et al.*, 1991), and this temperature was maintained throughout the observation period. Observation of specimens was performed by making use of the minimum dose system (MDS) (Fujiyoshi *et al.*, 1980), designed for recording high resolution images of radiation sensitive specimens with minimum electron exposure. Micrographs were recorded on Fuji FG film at magnifications of 20 000×−80 000× applying 1500−8800 electrons/nm^2, with an accelerating voltage of 400 kV and 8−11 s exposure, and the films were developed to an optical density of ~1.0 using Kodak D-19 developer at full strength. Beam damage within a specimen was examined by taking a series of four to five micrographs of the same observation field, successively applying 4000 electrons/nm^2 for each photograph (data not shown). The threshold dose for detectable damage in the specimens was 12 000 electrons/nm^2 at the present acceleration voltage of 400 kV and at a stage temperature of 4.2 K. Therefore, our cryo-stage allows us to take undamaged images of influenza virus embedded in ice with relatively high dose exposure such as 4000 electrons/nm^2.

Densitometric traces of the membrane region of the virus particles were taken from enlarged positive images on Sakura graphic art film by a Rigaku Model OS densitometer.

Assay of biological activities of influenza virus

Infectivity of the virus in the fractions obtained by Sephacryl S-1000 chromatography was tested by plaque assay on chick embryo fibroblasts according to the method of Klenk *et al.* (1975). Low pH induced fusion activity was assayed as in Stegmann *et al.* (1985) using human erythrocyte ghosts. HA titer and hemolysis activity were determined according to Salk (1944) and Sato *et al.* (1984), respectively, using human erythrocytes. Protein concentration was determined by the method of Lowry *et al.* (1951). Using the method of Bartlett (1959), the amount of lipid was determined in the lipid extract prepared as in Bligh and Dyer (1959). SDS−PAGE was performed according to Laemmli (1970) and quantification of the result was done by the dye-extraction method (Fenner *et al.*, 1975).

Acknowledgments

We would like to express sincere thanks to Drs Peter Tulloch, Ken Nishikawa, Yoshinobu Okuno and Sakuji Toyama for discussions and suggestions, and Drs Peter Tulloch and Aline Vertut-Doi for critical reading of the manuscript.

References

Adrian,M., Dubochet,J., Lepault,J. and McDowall,A.W. (1984) *Nature*, **289**, 32−36.

Bächi,T., Gerhard,W., Lindenmann,J. and Muhleethaler,K. (1969) *J. Virol.*, **4**, 769−776.

Bartlett,G.R. (1959) *J. Biol. Chem.*, **243**, 466−468.

Bligh,E.G. and Dyer,W.J. (1959) *Can. J. Biochem. Physiol.*, **37**, 911−917.

Booy,F.P., Ruigrok,R.W.H. and van Bruggen,E.F.J. (1985) *J. Mol. Biol.*, **184**, 667−676.

Brand,C.M. and Skehel,J.J. (1972) *Nature*, **238**, 145−147.

Bucher,D.J., Kharitonenkov,I.G., Zakomiridin,J.A., Grigoriev,V.B., Klimenko,S.M. and Davis,J.F. (1980) *J. Virol.*, **36**, 586−590.

Cevc,G. and Marsh,D. (1987) In Bittar,E.E. (ed.), *Cell Biology—Phospholipid Bilayers—Physical Principles and Models*. Wiley-Interscience Publishers, John Wiley and Sons, Vol. 5, pp. 1−56.

Colman,P.M., Varghese,J.N. and Laver,W.G. (1983) *Nature*, **303**, 41−44.

Compans,R.W., Klenk,H.D., Caliguli,L.A. and Choppin,P.W. (1970) *Virology*, **42**, 880−889.

Fenner,C., Traut,R.R., Mason,D.T. and Wikman-Coffelt,J. (1975) *Anal. Biochem.*, **63**, 595−602.

Fujiyoshi,Y., Kobayashi,T., Ishizuka,T., Uyeda,N., Ishida,Y. and Harada,Y. (1980) *Ultramicroscopy*, **5**, 459−468.

Fujiyoshi,Y., Uyeda,N., Yamagishi,M. Morikawa,K., Mizusaki,T., Aoki,Y., Kihara,H. and Harada,Y. (1986) *Proceedings of the XIth International Congress on Electron Microscopy*. pp. 1829−1832.

Fujiyoshi,Y., Mizusaki,T., Morikawa,K., Yamagishi,H., Aoki,Y., Kihara,H. and Harada,Y. (1991) *Ultramicroscopy*, **38**, 241−251.

Fuller,S.D. (1987) *Cell*, **48**, 923−934.

Gething,M.J., McCammon,K. and Sambrook,J. (1986) *Cell*, **46**, 939−950.

Gregoriades,A. (1980) *J. Virol.*, **36**, 470−479.

Herrero-Uribe,L., Mann,G.F., Zuckermann,A.J., Hockley,D. and Oxford,J.S. (1983) *J. Gen. Virol.*, **64**, 471−475.

Ishizuka,K. and Uyeda,N. (1977) *Acta Crystallogr.*, **A33**, 740−749.

Klein,P., Kanehisa,M. and DeLisi,C. (1985) *Biochim. Biophys. Acta*, **815**, 468−476.

Klenk,H.D., Rott,R., Orlich,M. and Blodron,J. (1975) *Virology*, **68**, 426−439.

Kyte,J. and Doolitle,R.F. (1982) *J. Mol. Biol.*, **157**, 105–132.
Laemmli,U.K. (1970) *Nature*, **227**, 680–685.
Lamb,R.A. and Choppin,P.W. (1983) *Annu. Rev. Biochem.*, **52**, 467–506.
Levine,Y.K. and Wilkins,M.H.F. (1971) *Nature New Biol.*, **230**, 69–72.
Lowry,O.H., Rousenbrough,N.Y., Farr,A.L. and Randall,R.J. (1951) *J. Biol. Chem.*, **193**, 265–275.
Maeda,T. and Ohnishi,S. (1980) *FEBS Lett.*, **122**, 283–287.
Nermut,M.V. (1972) *J. Gen. Virol.*, **17**, 317–331.
Nishikawa,K. and Ooi,T. (1986) *J. Biochem.*, **100**, 1043–1047.
Oxford,J.S. and Hockley,D.J. (1987) In Nermut,M.V. and Steven,A.C. (eds), *Animal Virus Structure—Orthomyxoviridae*. Elsevier, Amsterdam, pp. 213–232.
Pons,M.W., Schultze,I.T., Hirst,G.K. and Hanser,R. (1969) *Virology*, **39**, 250–259.
Sato,S.B., Kawasaki,K. and Ohnishi,S. (1984) *Proc. Natl Acad. Sci. USA*, **80**, 3153–3157.
Salk,J.E. (1944) *J. Immunol.*, **49**, 87–98.
Skehel,J.J. and Schild,G.C. (1971) *Virology*, **44**, 396–408.
Stegmann,T., Hoekstra,D., Scherphof,G. and Wilshut,J. (1985) *Biochemistry*, **24**, 3107–3113.
Szoka,F.,Jr and Papahadjopoulos,D. (1978) *Proc. Natl Acad. Sci. USA*, **75**, 4194–4198.
Wiley,D.C., Wilson,I.A. and Skehel,J.J. (1981) *Nature*, **289**, 366–373.
Winter,G. and Fields,S. (1980) *Nucleic Acids Res.*, **8**, 1965–1974.
Wrigley,N.G., Brown,E.B. and Skehel,J.J. (1986) In Harris,J. and Horne,R. (eds.), *Electron Microscopy of Proteins—Viral Structure*. Academic Press, London, Vol. 5, pp. 103–164.

Received on August 16, 1993; revised on October 11, 1993